The Physics of Thermonuclear Flames on Small Scales

R. Rosner,* N. Vladimirova, and D. Lamb†
ASCI Flash Center, Enrico Fermi Institute, The University of Chicago, 5640 South Ellis Avenue, Chicago, IL 60637

PACS numbers:

The feedback of a propagating diffusive (pre-mixed combustion) flame on a fluid, and the consequences for the flame, is of considerable interest in many areas of research. In our case, we have been motivated by the problem of the speedup of nuclear reaction fronts of this type in the interior of white dwarf stars, which is thought to be one possible way that such stars undergo thermonuclear disruption, e.g., a Type Ia supernova (cf. [1–6]). It is usual in this field to focus on the speedup of such flames for prescribed flows, with substantial recent advances [7]. For this "kinematic" problem, the goal is rigorous limits on flame speedup in the case in which there is no feedback onto the flow. The Type Ia supernova problem demands more than this, however: hence, we report progress on studies of the simplest case of feedback, namely that which occurs when a flame propagates vertically, against the direction of gravity. It is generally believed that under such circumstances, the flame front is likely to become distorted by Rayleigh-Taylor instability, and thus achieves speedup; previous calculations have been largely illustrative, and based upon fully-compressible fluid dynamics model (e.g., [8]) and fairly realistic nuclear reaction networks. Our approach instead looks at a much simpler problem, in which these "realistic" complexities are simply removed; the motivation is to strip the flame speedup problem to its bare essentials. For this reason we have studied flames in the Boussinesq limit and for highly simplified reaction terms; thus, we isolate the various effects which lead to flame speedup in the astrophysical context, allowing us to connect such simulations to extant analytical work (e.g., [7, 9, 10]), and to elucidate simple scaling laws (which suggest further analytical studies). Here we briefly describe some of our main results, details of which can be found elsewhere [11].

Our starting point is the coupled set of Navier-Stokes and advection-diffusion-reaction equations, written in the Boussinesq limit,

$$\begin{aligned} \rho\left[\frac{\partial \mathbf{v}}{\partial t} + (\mathbf{v}\cdot\nabla)\mathbf{v}\right] &= -\nabla p + \mu\nabla^2\mathbf{v} + \rho\mathbf{g}, \\ \frac{\partial T}{\partial t} + \mathbf{v}\cdot\nabla T &= \kappa\nabla^2 T + R(T), \\ \nabla\cdot\mathbf{v} &= 0, \end{aligned} \tag{1}$$

where $\mathbf{v}$ is the fluid velocity and, without loss of generality, the temperature T has been normalized to satisfy $0 \le T \le 1$. The thermal diffusivity κ and viscosity μ are assumed to be temperature-independent, and density (ρ) variations are assumed to be small enough to be described by the Boussinesq model, e.g., $\rho(T) = \rho_\circ + (\Delta\rho/\rho_\circ)T$. In the spirit of maintaining simplicity, we consider a reaction term of Kolmogorov-Petrovskii-Piskunov (KPP) type [12], of the form $R(T) = \alpha T(1-T)/4$, where α is the (laminar) reaction rate. This reaction form has an unstable fixed point at $T = 0$, the "unburned" state, and a stable one at $T = 1$, the "burned" state. Thus a fluid element with positive temperature will inevitably evolve to the burned state in a characteristic time of order $1/\alpha$. As is well-known from the combustion literature, the temperature equation from the system above admits — for a stationary fluid, and in the absence of gravity — one-dimensional solutions in the form of burning fronts propagating with laminar burning speed $s_\circ = \sqrt{\alpha\kappa}$, and with characteristic flame thickness $\delta = \sqrt{\alpha/\kappa}$. If it is further assumed that $T \to 1$ as $y \to -\infty$, and $T \to 0$ as $y \to +\infty$, then the front propagation is in the positive y direction. If the front thickness δ and the inverse reaction rate α^{-1} are put as the units of distance and time, respectively, the problem control parameters are the Prandtl number $\mathrm{Pr} = \frac{\nu}{\kappa}$ and the non-dimensional gravity $G = g\left(\frac{\Delta\rho}{\rho_\circ}\right)\frac{\delta}{s_\circ^2}$, where ν is a kinematic viscosity $\nu = \mu/\rho_\circ$. In addition, the system is characterized by a number of length scales specifying the initial state, which are in our case the dimensionless amplitude $A = a/\delta$ and the dimensionless wavelength $L = l/\delta$ of the initial flame front perturbation, $f(x) = a\cos(2\pi x/l)$, The vertical size of the computational domain was kept large so as to avoid effects due to the upper and lower walls of the computational box; in all cases, we have verified that such artifacts are not present. For this reason, the box height does not enter as a problem parameter. The initial velocities are set to zero, and most computations were carried out for $\mathrm{Pr} = 1$. The resolution of the simulations was chosen to fully resolve the laminar flame structure, as well as both the diffusive and viscous scales; for the KPP reaction term, the laminar flame thickness is approximately $12\,\delta$, the grid spacing $\Delta x = \Delta y = 1$ (in the units of δ), and the domain size up to 512×4096 for most computations. A typical initial state of our flame calculation is shown in Fig. 1. (Details regarding the simulations themselves can be found in [11].) Our central interest will be in disentangling the dependence of the flame behavior on the key control parameters of the problem.

*also at Depts. of Astronomy & Astrophysics and Physics The University of Chicago, Chicago, IL 60637
†also at Dept. of Astronomy & Astrophysics, The University of Chicago, Chicago, IL 60637

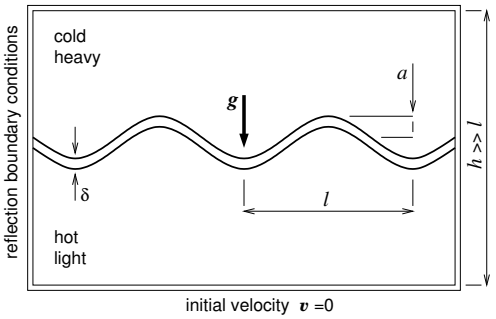

FIG. 1: A typical initial state of a flame calculation.

For a wide range of parameters, we can observe traveling waves of the temperature distribution, propagating with constant speed. Depending on simulation parameters, the initial perturbation either damps (e.g., the flame front flattens) or forms a curved front. The flat front moves in the motion-free (in the Boussinesq limit) fluid, has laminar front structure, and propagates with the laminar front speed. A typical curved front is shown in Fig. 2; it has the wavelength of the initial perturbation and is characterized by narrow dips (lower apexes), where the cold fluid falls into the hot region, and by wide tips (upper apexes), where buoyant hot fluid rises into the cold fluid. In the initial stages, the evolution pattern is similar to bubble and spike formation during the Rayleigh-Taylor instability [14, 15]; but in later stages, small scale structures are consumed by the flame, and, finally, the flame evolves toward the travelling wave solution shown in Fig. 2. The shape of the stable front is determined by gravity, G, and wavelength, L, and can be characterized by two vertical length scales associated with the spatial temperature variation (h_T) and the spatial velocity variation (h_V) of the flame. The speed of the curved front is always higher than the laminar flame speed, because of the increase in the flame front area and transport. Finally, we notice that the streamlines in Fig. 2 indicate that the flow underlying the propagating flame is characterized by rolls propagating upward.

One of our primary interests is to quantify the effects of variations in wavelength and gravity on the flame speed. It is convenient to define the speed of the travelling wave flame by the bulk burning rate [7], $s(t) = \frac{1}{l}\int_0^l \frac{\partial T(x,y,t)}{\partial t}\, dx\, dy$; this definition has the considerable advantage that it reduces to the standard definition of the flame speed when the flame is well-defined, and it is accurate to measure even for cases where the burning front itself is not well-defined. Henceforth we refer to it simply as the flame speed.

Our first result (shown in Fig. 3) is that the flame speed increases with wavelength L and with the gravitational acceleration G, and is independent of the initial perturbation amplitude A. More specifically, the flame becomes planar and moves at the laminar speed ($s = s_\circ$) if G is smaller than some critical value $G_{\rm cr}$; if G lies above

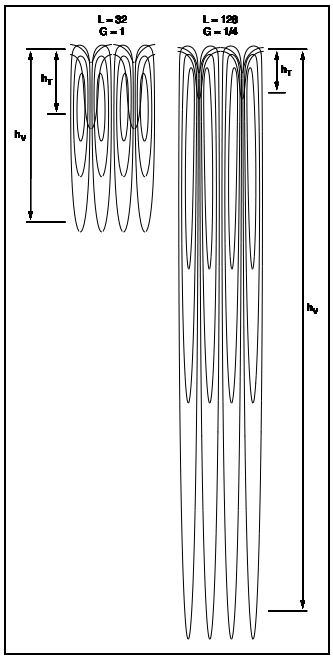

FIG. 2: Travelling wave isotherms ($T = 0.1$ and $T = 0.9$) and streamlines for two system with different simulation parameters. Note that the system on the right has been rescaled by a factor of 1/4 both horizontally and vertically.

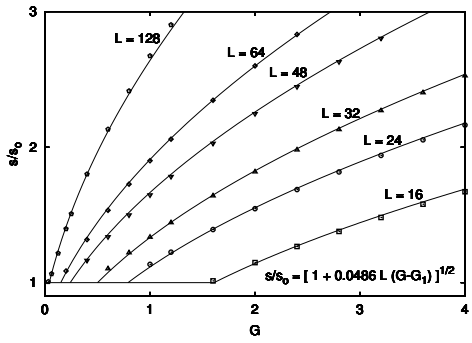

FIG. 3: Bulk burning rate (travelling wave speed) s as function of wavelength L for different values of gravity G.

this critical value, the flame speed can be fit by the expression, $s = s_\circ\sqrt{1 + k_1(G - G_1)L}$, where $k_1 \approx 0.0486$ is obtained from measurements derived from the simulation data. The second tuning parameter, G_1, was found to be a function of the perturbation wavelength (Fig. 4), $G_1 = 8(2\pi/L)^{1.72}$. For a relatively wide range of parameters, this expression describes experimental data well, but must be applied with caution near the cusp at $G = G_1$ shown in Fig. 3. Roughly speaking, this cusp can be interpreted as the transition between the planar and curved flame regimes, $G_1 \approx G_{\rm cr}$; closer investigation of the transition region shows that $G_{\rm cr} < G_1$, and that the fit (Fig. 3) underestimates the flame speed in this

transition region (Fig. 5).

The behavior near the transition is discussed in detail by Berestycki, Kamin & Sivashinsky [10], who derive the one-dimensional evolution equation for the front interface $y(x)$ and prove the following properties of $y(x)$, relevant to our case: (1) the existence of $G_{\rm cr} \sim (2\pi/L)^2$ such that there is no nontrivial solution for $G < G_{\rm cr}$ (i.e. the front is flat for $G < G_{\rm cr}$); (2) the existence of ${G_{\rm cr}}^* = 4G_{\rm cr}$ such that for $G > {G_{\rm cr}}^*$ there are two symmetrical (curved) solutions $y^+(x)$ and $y^-(x)$ which are stable, and any other solution including the trivial is unstable; (3) metastability of any solution except $y^+(x)$ and $y^-(x)$ in the range $G_{\rm cr} < G < {G_{\rm cr}}^*$, and convergence of this metastable solution to either $y^+(x)$ or $y^-(x)$. Also, based on the derivation in [10], it can be shown that the flame speed in the metastable regime scales as follows [16], $(s/s_\circ - 1) \propto (G - G_{\rm cr})^2$ as $(G - G_{\rm cr}) \to 0$. Our simulations confirm the dramatic increase of stabilization times close to the critical gravity value $G_{\rm cr}$. For this reason, it is very difficult to obtain reliable results regarding the flame speed in this transition regime. Even detecting the critical point takes significant computational effort (Fig. 5); measuring the velocity, which in this parameter regime differs from $s_\circ$ by a very small amount, is harder still. However, the transition is sharper and is easier to see when studying the vertical distance between the upper and lower apexes of the flame, h_T, measured by the expression, $h_T = \int_{-\infty}^{\infty} (T(0) - T(l/2))\, dy$. In the limit of large wavelengths ($L \gg 1$), the transition occurs at small values of gravity, and the flame speed is determined by a single parameter, the product LG. If, in addition, the product LG is large, the flame speed scales as $s/s_\circ \approx 0.22\sqrt{LG}$. This result is in good agreement with the rising bubble model [17] which, in the Boussinesq limit, predicts $s/s_\circ = \sqrt{LG/6\pi} \approx 0.23\sqrt{LG}$ for a 2-D open bubble [18]. We further observe that in the large wavelength limit, the h_T/l ratio obeys the same scaling (Fig. 5).

We note that the flame structure shares features of flame propagation from both shear and cellular flow. For instance, the temperature distribution closely resembles that of a flame distorted by a shear flow, while the velocity distribution resembles that inside an infinitely tall cell. The flame speed in the shear and cellular flow is determined by the flow speed and by the length scale of the flow (period of shear or cell size) [19]. In particular, in both cases the flow speed scales with maximum flow velocity as $s \propto v_{max}^n$, with $n = 1$ for burning in the shear flow and $n = 1/4$ for burning in the cellular flow. Similarly, we have tried to determine whether the flame speed relates to the maximum velocity of the flow when flow and flame are coupled through the Boussinesq model. The available data (shown in Fig. 6) do not demonstrate a power law dependence with a single well-defined power. Furthermore, the dependence on L is not as dramatic as in the cases of shear or cellular flows.

To summarize, we have studied the fully nonlinear behavior of diffusive pre-mixed flames in a gravitationally stratified medium, subject to the Boussinesq approximation. Our aim was both to compare our results for a viscous system with analytical (and empirical) results in the extant literature, and to better understand the phenomenology of fully nonlinear flames subject to gravity. The essence of our results is that there is an extended regime for flames with finite flame front thickness for which the scaling on the LG product applies (as it is

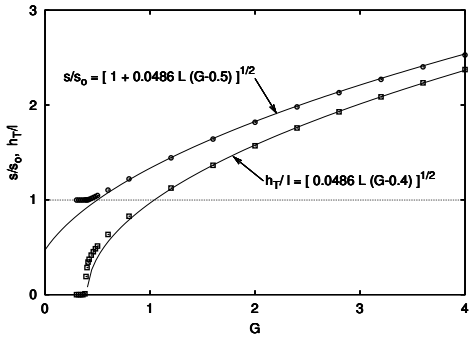

FIG. 5: Amplitude of the stable front as function of gravity for the wavelength $L = 32$. The scaling relations shown here are discussed in the text.

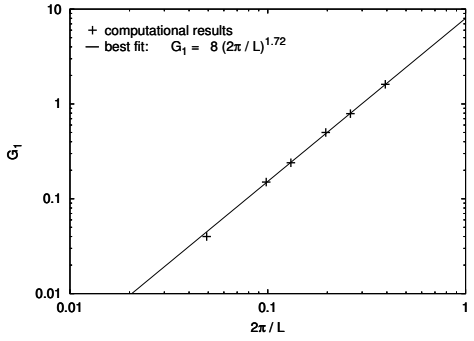

FIG. 4: Transitional point G_1 as a function of wavelength.

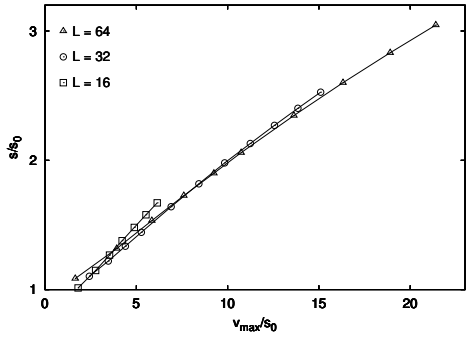

FIG. 6: The flame speed as function of maximal flow velocity.

known to do in the thin flame front limit).

Acknowledgements. This work was supported by the Department of Energy under Grant No.B341495 to the Center for Astrophysical Thermonuclear Flashes at the University of Chicago. We would like to thank helpful discussions with P. Constantin, L. Ryzhik, and O. Ruchayskiy.

[1] Whelan, J., & Iben, I., ApJ, **186**(3), 1007-1014 (1973).
[2] Livne, E., ApJ, **406**, L17 (1993).
[3] Khokhlov, A.M., ApJ, **449**, 695 (1995).
[4] Niemeyer, J.C., & Hillebrandt, W., ApJ, **452**, 779 (1995).
[5] Reinecke, M., Hillebrandt, W., & Niemeyer, J.C., A&A, **347**(2), 724 (1999).
[6] Gamezo, V.N., Khokhlov, A.M., & Oran, E.S., BAAS **200**, 1401 (2002).
[7] Constantin, P., Kiselev, A., Oberman, A., & Ryzhik, L., Arch. Rat. Mech. Anal. **154**, 53 (2000).
[8] Röpke, F.K., Hillebrandt, W., & Niemeyer, J.C., astro-ph/0204036 (2002).
[9] Audoly, B., Berestycki, H., & Pomeau, Y., C.R.Acad. Sci., Ser. IIB **328**, 255 (2000).
[10] Berestycki, H., Kamin, S., & Sivashinsky, G., Interfaces and Free Boundaries **3**, 361 (2001).
[11] Vladimirova, N., & Rosner, R., Phys. Rev. E, in press (2003).
[12] Kolmogorov, A.N., Petrovskii, I.G., & Piskunov, N.S., Bull. Moskov. Gos. Univ. Mat. Mekh. **1** (1937), 1-25 (see [20] pp. 105-130 for an English translation).
[13] Young, Y.-N., Tufo, H., Dubey, A., & Rosner, R., JFM, **447**, 377 (2001).
[14] Chandrasekhar, S., *Hydrodynamic and Hydromagnetic Stability*, Clarendron Press, Oxford, (1961).
[15] Landau, L.D., & Lifshitz, E.M., *Fluid Mechanics*, 2nd edition, Pergamon Press, Oxford, (1987).
[16] Kiselev, A., & Ryzhik, L., private communication.
[17] Bychkov, V.V., & Liberman, M.A., Physics Reports **325**, 115 (2000).
[18] Layzer, D., ApJ, **122**, 1 (1955).
[19] Vladimirova, N., Constantin, P., Kiselev, A., Ruchayskiy, O., & Ryzhik, L., physics/0212057 (2002).
[20] *Dynamics of Curved Fronts*, Pelcé, P., Ed., Academic Press (1988).